THIS REPORT HAS BEEN DELIMITED
AND CLEARED FOR PUBLIC RELEASE
UNDER DOD DIRECTIVE 5200.20 AND
NO RESTRICTIONS ARE IMPOSED UPON
ITS USE AND DISCLOSURE.

DISTRIBUTION STATEMENT A

APPROVED FOR PUBLIC RELEASE;
DISTRIBUTION UNLIMITED.

AD 72938

Armed Services Technical Information Agency

Reproduced by

DOCUMENT SERVICE CENTER

KNOTT BUILDING, DAYTON, 2, OHIO

NOTICE: WHEN GOVERNMENT OR OTHER DRAWINGS, SPECIFICATIONS OR OTHER DATA ARE USED FOR ANY PURPOSE OTHER THAN IN CONNECTION WITH A DEFINITELY RELATED GOVERNMENT PROCUREMENT OPERATION, THE U. S. GOVERNMENT THEREBY INCURS NO RESPONSIBILITY, NOR ANY OBLIGATION WHATSOEVER; AND THE FACT THAT THE GOVERNMENT MAY HAVE FORMULATED, FURNISHED, OR IN ANY WAY SUPPLIED THE SAID DRAWINGS, SPECIFICATIONS, OR OTHER DATA IS NOT TO BE REGARDED BY IMPLICATION OR OTHERWISE AS IN ANY MANNER LICENSING THE HOLDER OR ANY OTHER PERSON OR CORPORATION, OR CONVEYING ANY RIGHTS OR PERMISSION TO MANUFACTURE, USE OR SELL ANY PATENTED INVENTION THAT MAY IN ANY WAY BE RELATED THERETO.

UNCLASSIFIED

AD No. 72938
ASTIA FILE COPY

ENGINEERING EXPERIMENT STATION

UNIVERSITY OF ILLINOIS

FC

INTERIM PROGRESS REPORT

FEBRUARY 1, 1954 THROUGH JUNE 30, 1955

I. The "equivalent reaction pair" approach to the study of complex electrode reaction mechanisms.

II. Experimental methods for the study of the degree of corrosion of phosphide electrodes.

III. Results obtained from the corrosion studies of phosphide anodes and discussion of these results.

IV. Theory of "faradaic rectification" and a discussion of possible applications of the phenomenon.

V. Experimental technique for the study of faradaic rectification and results thereby obtained for a mercury electrode.

by

K. B. Oldham

Contract N6-ori-71, Task Order No. XI

Office of Naval Research, Department of the Navy

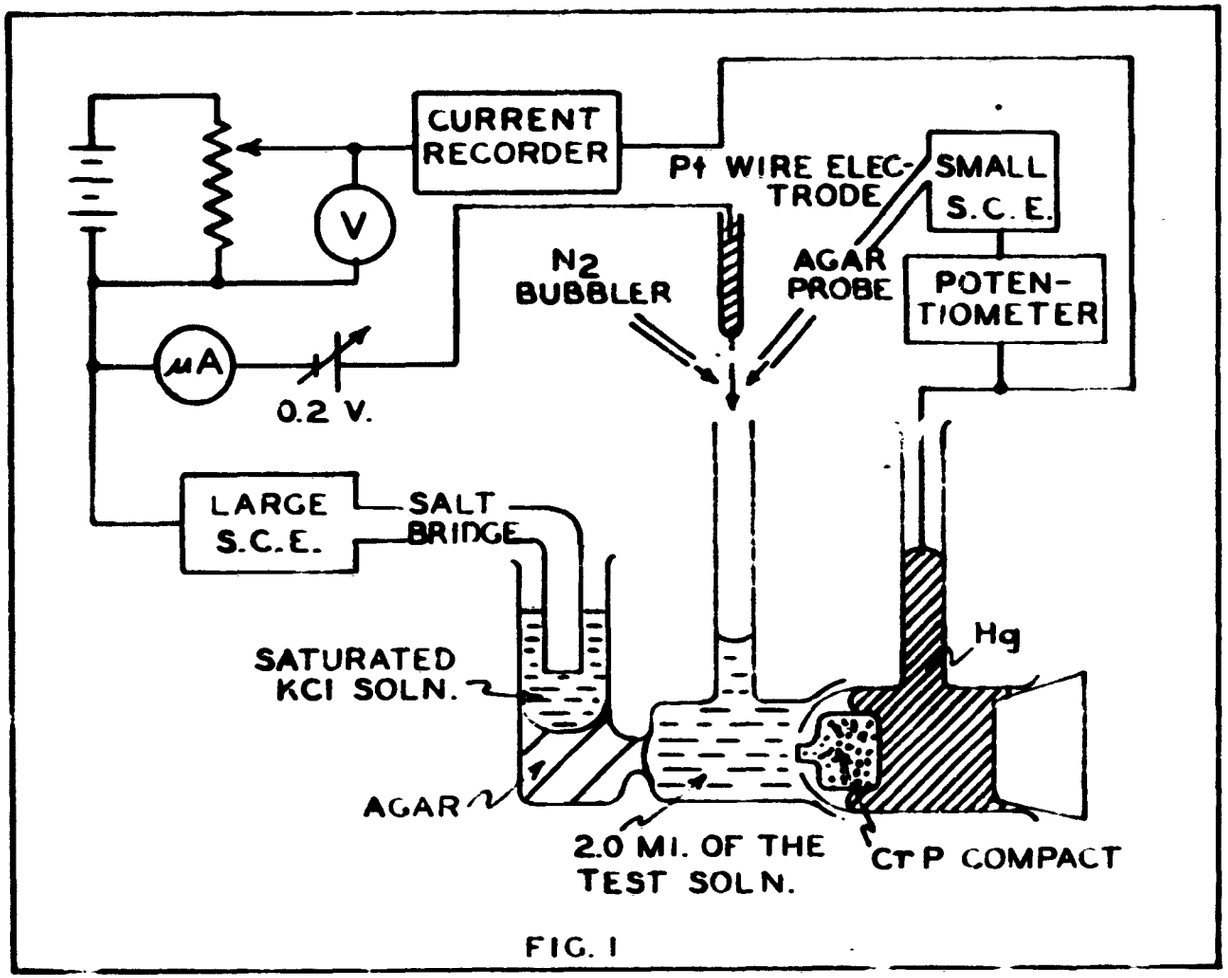
CURRENT RECORDER
Pt WIRE ELEC-TRODE
SMALL S.C.E.
V
N2 BUBBLER
AGAR PROBE
POTEN-TIOMETER
μA
0.2 V.
LARGE S.C.E.
SALT BRIDGE
Hg
SATURATED KCl SOLN.
AGAR
2.0 Ml. OF THE TEST SOLN.
Ct P COMPACT

FIG. 1

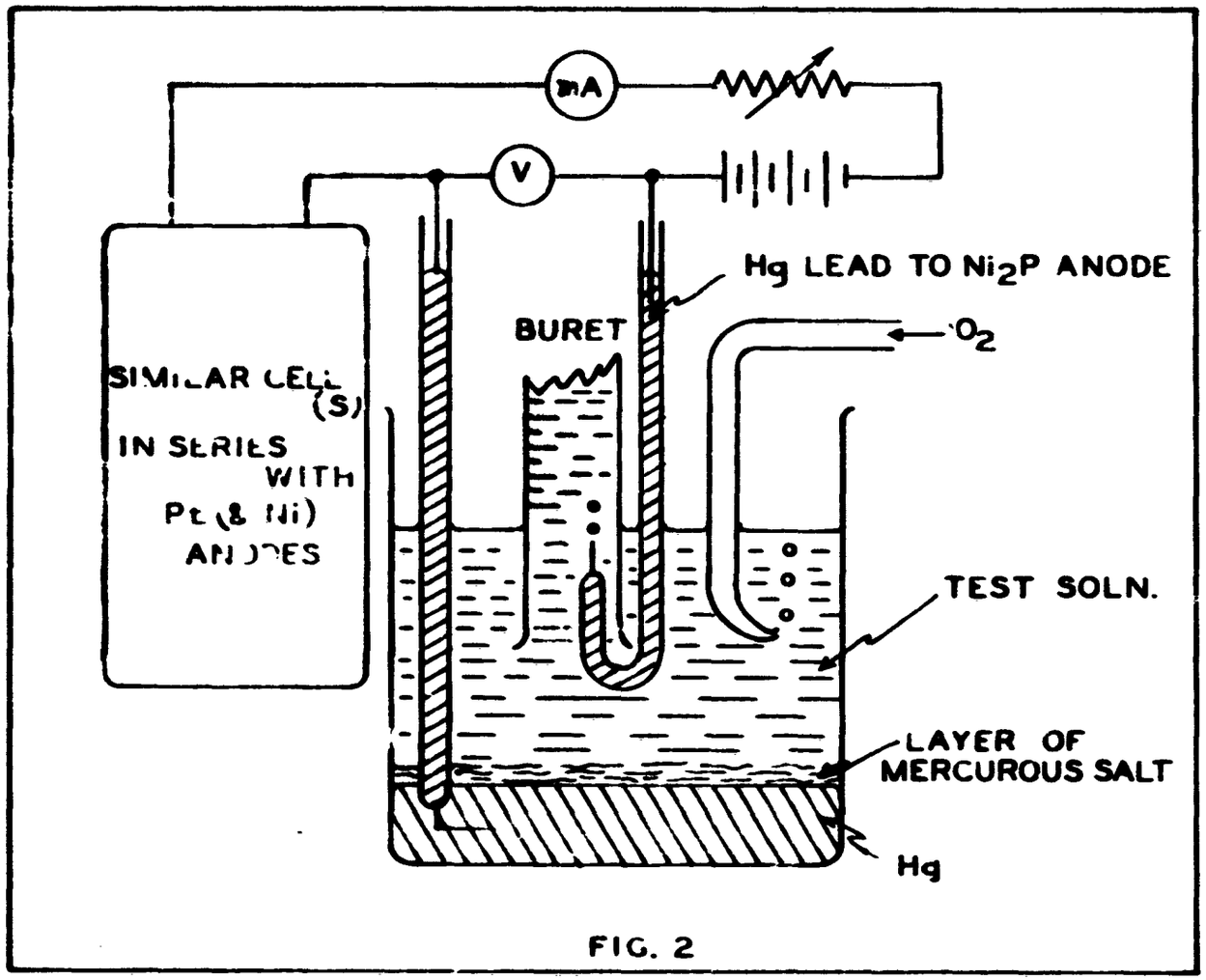
mA
V
Hg LEAD TO Ni_2P ANODE
BURET
O_2
SIMILAR CELL (S)
IN SERIES WITH
Pt (& Ni)
ANODES
TEST SOLN.
LAYER OF
MERCUROUS SALT
Hg

FIG. 2

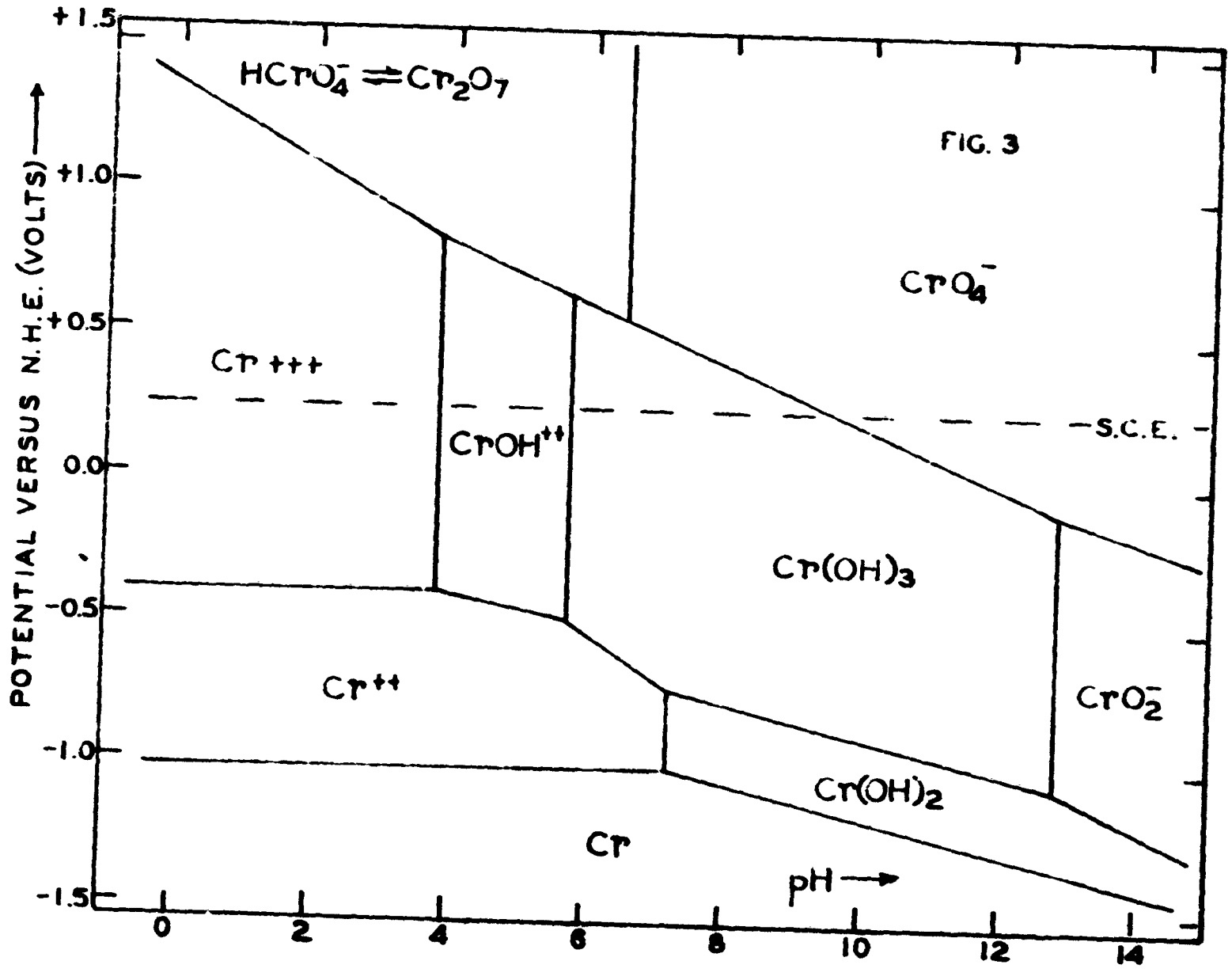
+1.5
+1.0
+0.5
0.0
-0.5
-1.0
-1.5
POTENTIAL VERSUS N.H.E. (VOLTS)
HCrO4- ⇌ Cr2O7
CrO4-
Cr+++
S.C.E.
CrOH++
Cr(OH)3
Cr++
CrO2-
Cr(OH)2
Cr
pH
0
2
4
6
8
10
12
14

FIG. 3

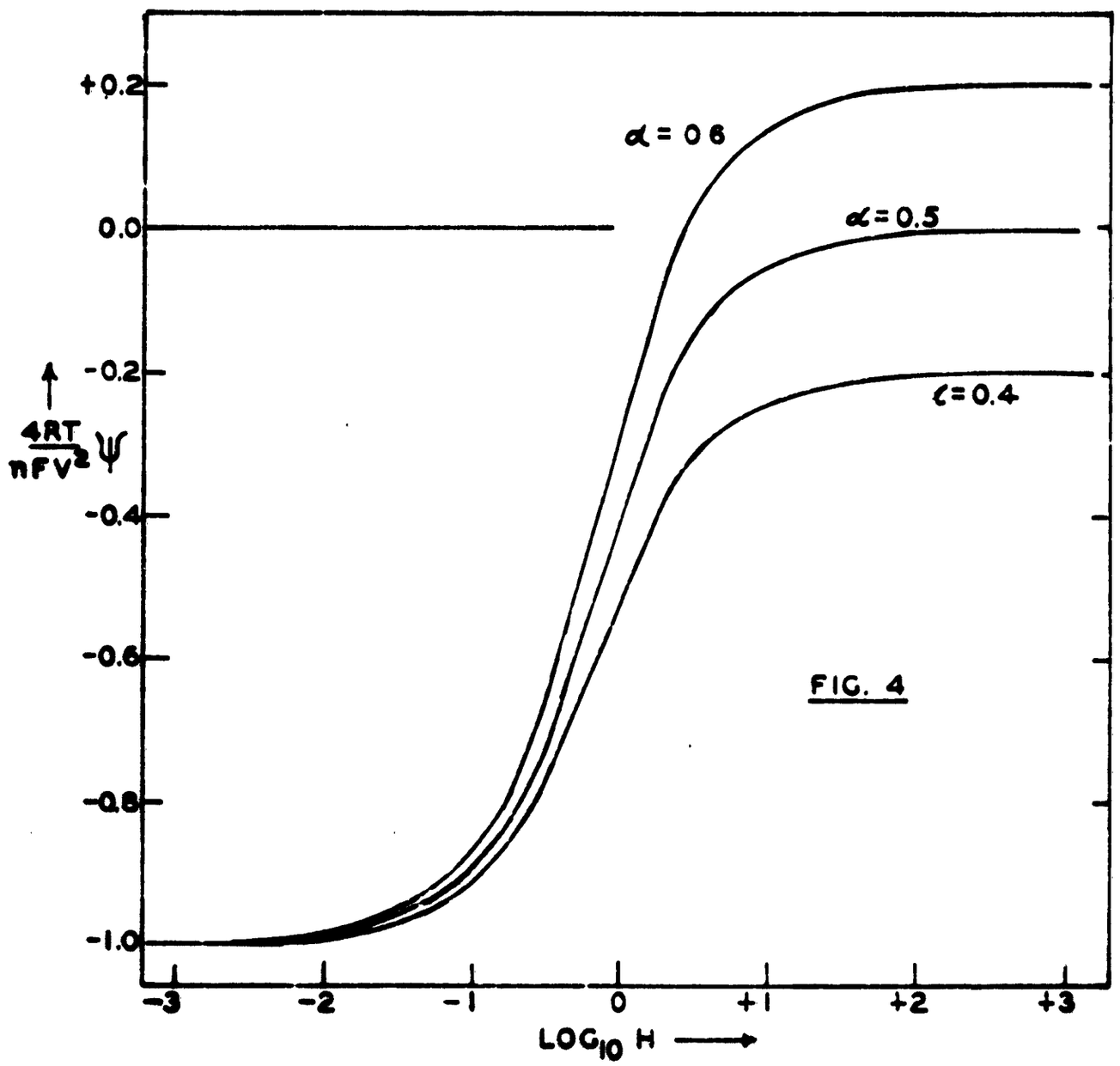
+0.2
0.0
-0.2
-0.4
-0.6
-0.8
-1.0
$\frac{4RT}{nFV^2}\psi$
$\alpha = 0.6$
$\alpha = 0.5$
$\alpha = 0.4$
-3
-2
-1
0
+1
+2
+3
LOG_{10} H

FIG. 4

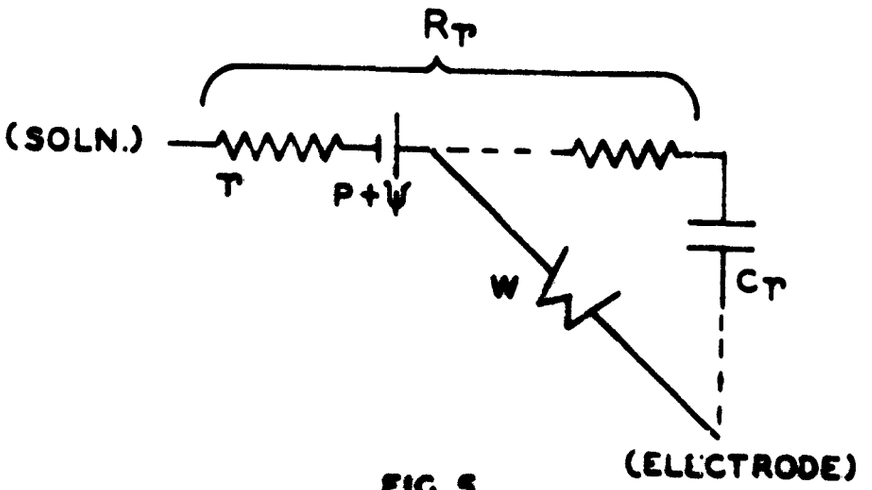

FIG. 5

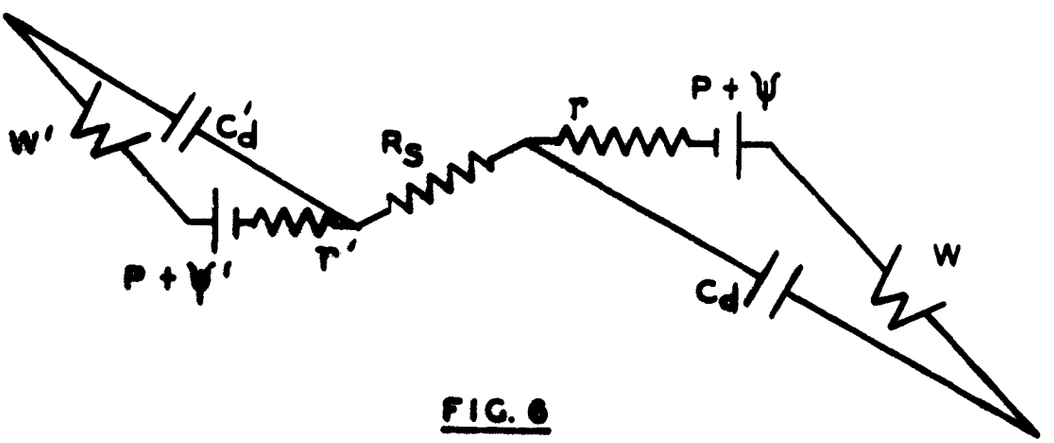

FIG. 6

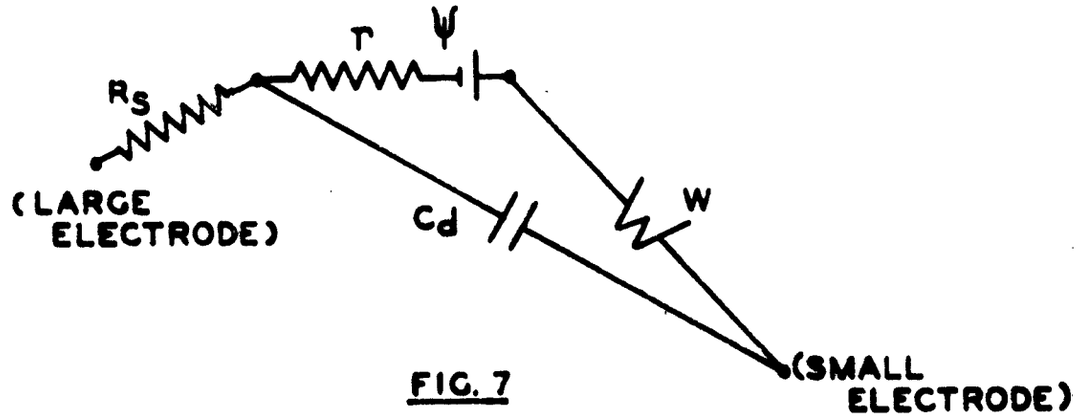
T
Ψ
R_S
(LARGE ELECTRODE)
C_d
W
(SMALL ELECTRODE)

FIG. 7

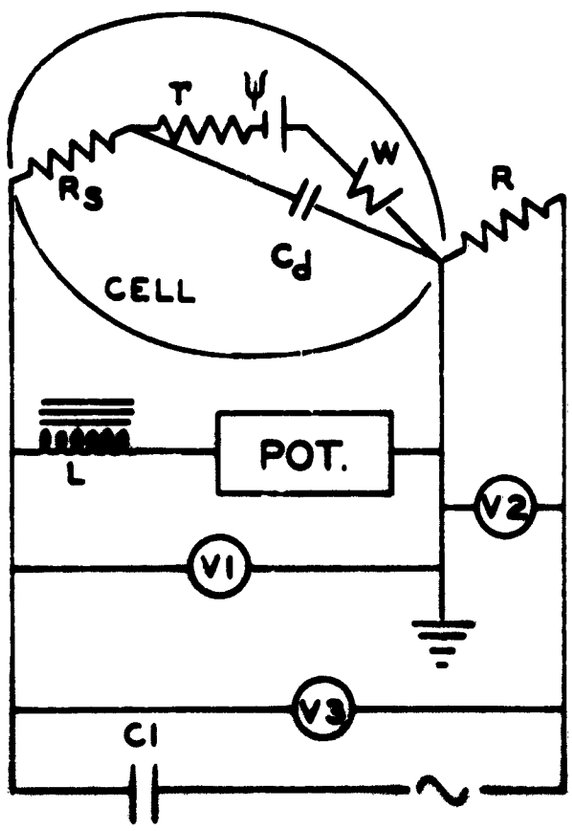
T
Ψ
W
R_S
R
C_d
CELL
L
POT.
V2
V1
V3
C1

FIG. 8

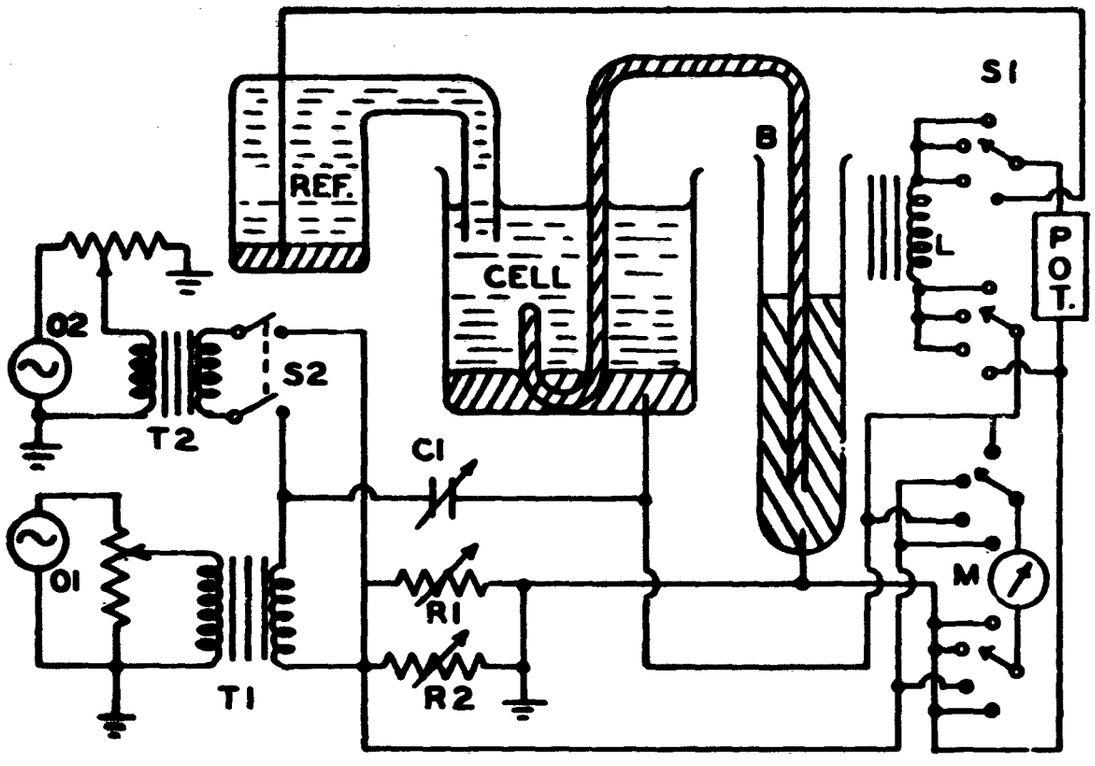

FIG. 9

DISTRIBUTION LIST

Copies		Copy No.
1	Office of Naval Research Branch (Boston)	1
1	Office of Naval Research Branch (Chicago)	2
1	Office of Naval Research Branch (New York)	3
1	Office of Naval Research Branch (San Francisco)	4
1	Office of Naval Research Branch (Pasadena)	5
2	Officer-in-Charge, Office of Naval Research	6-7
9	Director, Naval Research Laboratory	8-16
4	Chief of Naval Research, Chemistry Branch	17-20
1	Research and Development Board	21
1	Research and Development Division	22
1	Chemical and Plastics Section, RDB-MPD	23
1	Quartermaster Research and Development Command	24
1	Department of the Air Force	25
3	Department of the Army	26-28
1	Research and Development Group, Department of the Army	29
2	Naval Research Laboratory, Chemistry Division	30-31
2	Chief of the Bureau of Ships, Department of the Navy	32-33
2	Chief of the Bureau of Aeronautics	34-35
4	Chief of the Bureau of Ordnance	36-39
5	Armed Services Technical Information Agency	40-44
1	Signal Corps Engineering Laboratories	45
1	U. S. Naval Radiological Defense Lab	46
1	Naval Ordnance Test Station	47
1	Office of Ordnance Research	48
1	Technical Command, Chemical Corps	49
1	U.S. Atomic Energy Commission, Chemistry Division	50
1	U. S. Atomic Energy Commission, Research Division	51
1	U. S. Atomic Energy Commission, Library Branch	52
1	Horizons, Incorporated	53
1	Pennsylvania Salt Manufacturing Company	54
1	Providence College (Hackett and Fineman)	55
1	Department of Metallurgy, Mass. Institute of Technology	56
1	Chief of Naval Research, Armament Branch	57
1	Chief of Naval Research, Power Branch	58
1	University of North Carolina (Tyree)	59

The Engineering Experiment Station, University of Illinois

A CONCLUDING REPORT BY K. B. OLDHAM TO THE U. S. OFFICE OF NAVAL RESEARCH, DEPARTMENT OF NAVY, OF WORK CARRIED OUT BY HIM UNDER CONTRACT N6ori-071(50) - NR 356-341 DURING THE PERIOD FEBRUARY 1, 1954 THROUGH JUNE 30, 1955.

I. INTRODUCTORY REMARKS

The contract was established in July 1953 for the "preparation and electrochemical study of non-corrodible anodes". The primary purpose of these investigations has been the development of conducting materials that will satisfactorily resist corrosion when used as anodes in various aqueous solutions. Such substances would be potential substitutes for the noble metals which are extensively employed in electrochemical preparations. Previous researches[1, 2] showed that the phosphides of the transition metals had considerable promise as non-corrodible anodes and these compounds alone have been studied.

The role of the author in the investigations conducted under this contract has been the evaluation of phosphide samples with respect to their corrosion properties and the determination of the range of conditions, if any, under which each particular phosphide sample shows corrosion resistance. It was felt to be worthless to conduct electrochemical studies of phosphides in media in which chemical attack was suffered. Hsu, Yocom and Cheng[3] made experiments on phosphide samples in which the rate of weight loss was determined in various aqueous solutions.

The results of these experiments have been such that, up to the time of writing, only two phosphide samples have warranted electrochemical investigation.

At times when phosphide electrodes have not been available for corrosion tests, attention has been directed towards related aspects of electrochemistry. Methods of investigation have been developed which it is hoped will throw light on the mechanisms of anodic corrosion and of electrode reactions in general.

The subject of this report falls naturally into the following categories:

The "equivalent reaction pair" approach to the study of complex electrode reaction mechanisms.

Experimental methods for the study of the degree of corrosion of of phosphide electrodes.

Results obtained from the corrosion studies of phosphide anodes and discussion of these results.

Theory of "faradaic rectification" and a discussion of possible applications of the phenomenon.

Experimental technique for the study of faradaic rectification and results thereby obtained for a mercury electrode.

The material will be presented in the order listed above, but this should be understood to have no chronological significance.

II. COMPLEX ELECTRODE REACTIONS

A treatment has been devised that enables a complex electrode reaction to be reduced to a much simpler "equivalent reaction pair",

provided the reaction mechanism is known or can be postulated. From the equivalent reaction pair it is possible to predict current-voltage curves and all other properties that depend on the kinetics of the electrode reaction. The converse is only partially true: analysis of experimental results in terms of the treatment will enable certain mechanisms to be ruled out of consideration; however others will probably be left in dispute.

The mathematical derivation of the treatment will not be presented here, since this has been reported in full previously. Moreover, the material is in publication[4]. However, the example below, which is taken from the phosphide corrosion discussion of section IV of this report, will serve to illustrate the application and limitation of the equivalent reaction pair method.

The corrosion of a chromium phosphide anode in acid solution occurs with a stoichiometry which can be represented by the overall reaction:

$$2CrP + 15H_2O = Cr_2O_7^{--} + 2PO_4^{---} + 30H^+ + 22e^- \qquad (a)$$

Such an electrode reaction clearly warrants the term "complex". Equation (a) cannot possibly depict the mechanism, for it has a far greater molecularity than is feasible.

The number of mechanisms that may be envisaged to explain the overall reaction (a) is legion. For example, the following four steps may be imagined to occur:

$$CrP + 2H_2O = Cr^{+++} + H_2PO_2^- + 2H^+ + 4e^- \qquad (b)$$

$$Cr^{+++} + 4H_2O = CrO_4^{--} + 8H^+ + 3e^- \qquad (c)$$

$$H_2PO_2^- + 2H_2O = PO_4^{---} + 6H^+ + 4e^- \qquad (d)$$

$$2CrO_4^{--} + 2H^+ = Cr_2O_7^{--} + H_2O \qquad (e)$$

where reaction (b) is the rate-determining step in the sequence. Now, applying the method of the equivalent reaction pair, we may combine reactions (b) through (3) into (f), a hypothetical reaction pair which has all the kinetic attributes of the four reactions above, thus:

$$CrP + 2H_2O - (4-4\alpha)e^- = \tfrac{1}{2}Cr_2O_7^{--} + PO_4^{---} + 15H^+ - 5\tfrac{1}{2}H_2O + (7+4\alpha)e \qquad (f)$$

where α is a symmetry factor or transfer coefficient, taking some value between zero and unity.

Alternatively, the mechanistic scheme may be considered to consist of the following four reactions:

$$CrP + 5H_2O = Cr(OH)_2PO_2 + 8H^+ + 8e^- \qquad (g)$$

$$Cr(OH)_2PO_2 + 2H^+ = Cr^{+++} + PO_2^- + 2H_2O \qquad (h)$$

$$2Cr^{+++} + 7H_2O = Cr_2O_7^{--} + 14H^+ + 6e^- \qquad (i)$$

$$PO_2^- + H_2O = PO_4^{---} + 2H^+ \qquad (j)$$

and the corresponding equivalent reaction pair is found to be:

$$CrP - 6H^+ + 5H_2O - 8e^- = \tfrac{1}{8}Cr_2O_7^{--} + PO_4^{---} + 9H^+ - 2\tfrac{1}{8}H_2O + 3e^- \qquad (k)$$

if (h) is the slow step in the scheme.

It will be noted that hydrogen ions are absent from the left hand side of (f), whereas they are present with the coefficient -6 in (k). This is to be interpreted as meaning that corrosion (the left to right direction of reactions (a), (f) and (k)) will be unaffected by pH in case the scheme (b, c, d, e) represents the true course of the corrosion reaction, but if scheme (g, h, i, j) is correct increasing hydrogen ion concentration will have an inhibitive effect on corrosion.

The experimental results presented in section IV of this report show clearly that in the range pH 0 to pH 7, the intensity of corrosion is independent of hydrogen ion concentration. Thus scheme (g, h, i, j) cannot represent the mechanism. This is not to say that scheme (b, c, d, e) is correct, for any scheme that results in the absence of protons from the left hand side of the equivalent reaction pair (and there are very many that do) is equally acceptable. Such a conclusion is typical of most that will be given by the equivalent reaction pair approach. While it will often enable certain mechanisms to be rejected and suggest others, it will rarely give a decisive answer to a problem.

The above schemes (b, c, d, e) and (g, h, i, j) are purely illustrative and are not to be considered as serious attempts to explain the mechanism of the corrosion of phosphide anodes. Though they are considerably simpler than the overall reaction (a), not one of the reactions (b) through (j) is simple enough to be a likely primary unit of a mechanistic scheme. The problem of elucidating the mechanism of a corrosion reaction such as this is an extremely difficult one, complicated as it probably is by the

presence of one or more films. The corrosion reaction must also be considered in the light of its competitive reactions, such as solvent decomposition or anion discharge.

III. CORROSION EXPERIMENTS

Two phosphide samples were available for electrochemical corrosion tests: a short piece of nickel phosphide, Ni_3P, wire and a "slug" of compacted chromium phosphide, CrP. The latter compound is very refractory and compacts were prepared[3] by sintering the powdered material under argon.

Four avenues of approach to the determination of the degree of corrosion suggest themselves, viz:

(A) The measurement of the rate of weight loss at a measured current density.

(B) Measurement of the rate of accumulation of corrosion products.

(C) Measurement of the rate of liberation of the non-corrosion product (e.g. oxygen), whence the rate of corrosion may be determined by difference from the total current passed.

(D) Indirectly, by the analysis of current-voltage curves.

The potentialities of all these methods were studied.

Preliminary experiments showed that the exposed surface of anodically polarized phosphide samples underwent physical disintegration in addition to electrochemical corrosion. This was manifested by the deposition of a fine gray powder on the floor of the vessel adjacent to the anode and by visible "flaking" of the phosphide surface. It is believed that this disintegration is caused by the formation of gas bubbles inside the

surface layers of the anode, due to the appreciable porosity of the phosphide samples. This belief is supported by the observation of a higher degree of disintegration of CrP compared with the Ni_2P, in line with the greater porosity of the compacted material. Simple measurement of weight loss could not differentiate between this disintegration and true corrosion; (A) was therefore abandoned.

The corrosion of Ni_2P and CrP was found to yield the ions Ni^{++}, $Cr_2O_7^{--}$ and Cr^{+++}. Analysis of these ions is a comparatively simple matter and hence approach (B) was employed extensively. The experimental details of the various methods are given below. It was tacitly assumed that the phosphorus content of the anodes was corroded to the +5 state, i.e. to the PO_4^{---} ion or some similar phosphate anion.

The third approach, (C), offers a very simple and powerful method for assessing the degree of corrosion. By placing in series two cells, identical in all respects except that one has a phosphide anode and the other an inert electrode of the same area, a direct estimation of the extent of corrosion is obtained by comparison of the oxygen volumes liberated at each anode. This method was used extensively for Ni_2P anodes but could not be successfully employed for the CrP compacts, for the following reason. The method necessitates the passage of a considerable quantity of electricity in order that the gas volumes may be accurately compared. However, as noted above, the CrP compacts are very susceptible to physical disintegration and this results in a "paste" of loose powder, gas bubbles and solution being formed at the anode surface. Under such conditions the electrode area is indefinite and is subject to wild

fluctuations. To obviate this undesirable effect, it is necessary to obtain a measure of the degree of corrosion with the least possible passage of electricity. The (B) approach is the most favorable in this respect.

Results obtained with iron and cobalt phosphides[1,2] showed that the presence of corrosion was clearly reflected in current-voltage curves recorded with phosphide microanodes. However, no such correlation was found in the case of CrP. Method (D) was therefore considered to be unreliable and was abandoned.

Below are listed, in some detail, the experimental techniques actually used to provide the data listed in section IV.

Method 1 The cell shown in Fig. 1 was constructed. This consists of a chamber (of about 2 cm^3 volume) on one vertical wall of which a circular face(1 to 1 1/2 mm. in diameter) of the compact was exposed. The opposite face was an agar plug which was connected by a salt bridge to a saturated calomel cathode. The cell was filled with 2.00 mls of the solution under study. A small nitrogen bubbler could be inserted into the solution to prevent the ingress of atmospheric oxygen. The probe of a small potential-measuring calomel electrode was also inserted into the solution.

Preliminary experiments in a conventional cell showed that the dichromate ion in deoxygenated solutions of normal sulphuric acid gives a well-defined diffusion wave at a platinum wire microcathode. The half-wave potential was +0.47 volts vs S.C.E. ("European" convention) and the diffusion current (corrected for residual and measured at +0.2 volts) was accurately proportional to dichromate ion concentration.

A very simple method was thus available for the determination of the rate of corrosion of CrP in $\underline{N}$ H_2SO_4. A calibrated platinum wire electrode was inserted into the cell shown in Fig. 1 and, during the course of a corrosion experiment, measurements were made of the current drawn at +0.2 volts. Unfortunately, the characteristics of the platinum wire (in particular the residual current at +0.2 volts) were subject to a random variation of such a magnitude that this method of dichromate assay was subsequently abandoned.

Method 2 This method employed the cell shown in Fig. 1. After a known current had been passed for a known length of time, a single drop of the solution was withdrawn and treated with one drop of 1% ethanolic diphenylcarbazide (otherwise called diphenylcarbohydrazide, Ph.NH.NH.CO.NH.NH.Ph)[5]. This is a well-known spot test for the dichromate ion[6] and the method was made semi-quantitative by comparing the color with that given by a series of solutions with known dichromate ion content. Interpolation enabled a fairly accurate estimate to be made of the dichromate concentration.

Method 3 The previous spot-test method gives a measure only of the Cr(VI) content of the solution. However, in some cases as noted above, corrosion also occurs to Cr(III). The degree of corrosion to this state was estimated in the following manner. A portion of the solution was analysed for Cr(VI) in the usual way. A further portion was treated with potassium persulphate prior to analysis. By difference a measure of the Cr(III) concentration was obtained.

Method 4 A spot-test method was also applied to the analysis of solutions subjected to Ni_3P corrosion, but not as a quantitative procedure. The absence of colour on treatment with the well-known dimethylglyoxime reagent was taken as indicative of the complete absence of Ni^{++}.

Method 5 It has been noted above that in the case of Ni_3P cast anodes it was possible to use assay methods based upon the direct comparison of oxygen volumes liberated at an Ni_3P microanode and in a similar cell containing an inert metal microanode. When basic solutions were employed, three such cells were wired in series, equipped with Ni, Pt and Ni_3P anodes. For other solutions, only two series cells were employed, those with Pt and Ni_3P anodes. Anode areas were approximately 10^{-2} cm.^{2}

Fig. 2 is a diagram of the type of cell employed. The cell was simply a beaker containing the solution through which was bubbled a slow but continuous stream of oxygen. The floor of the beaker was covered with a layer of mercury topped by a layer of an appropriate mercurous salt (e.g. Hg_2SO_4 for Na_2SO_4 solution and Hg_2O for KOH). The anodes were short lengths of wire which were waxes into the end of the shorter limb of a J-shaped glass tube. Contact was established through a column of mercury and a burette was inverted over the anode and filled with solution. By assuming that the oxygen current efficiency at Pt (and Ni for alkaline solutions) was 100%, the degree of corrosion was readily obtained from the difference in oxygen volumes after electrolysis.

Method 6 Corrosion experiments conducted upon CrP at high current density produced dichromate ion at a concentration great enough for classical methods of analysis. The entire cell contents, following a corrosive electrolysis, were titrated iodometrically with a sodium thiosulphate solution which had been previously standardised with a potassium dichromate solution of known concentration.

Method 7 Spectrophotometry of $Cr_2O_7^{--}$ can be quite accurate for concentrations as low as 10^{-5} M. A method was developed in which the contents of the cell shown in Fig. 1 were compared with similar solutions of known dichromate concentration, using a Beckman Model D.U. Spectrophotometer at 350 millimicrons, the wavelength of maximum absorption.

The above seven methods were all employed to determine the extent of corrosion of CrP and Ni_2P in various solutions. In addition, some experiments were performed in an attempt to elucidate the nature of the corrosive attack. These latter are described in the next section.

IV. RESULTS OF CORROSION STUDIES

The degree of corrosion of an anode in a particular experiment has been expressed as a percentile "corrosion efficiency". This is defined as the percentage of the total current passed that is effective in causing corrosion. In terms of corrosion products, if micro moles of product accumulate in t seconds, through the passage of a current, i, in milliamperes, then:

Corrosion efficiency = $9650\frac{nM}{it}$ % where n is the number of electrons associated with the liberation of one ion of the corrosion

product. Thus for the production of Ni^{++} ions from the corrosion of Ni_3P, n = 4.5, since the reaction is:

$$Ni_3P + 4H_2O = 3Ni^{++} + PO_4^{---} + 8H^+ + 9e^-$$

For corrosion of CrP to dichromate, n = 22, whereas n = 8 if the corrosion product is Cr^{+++}. The corresponding reactions are:

$$2CrP + 15H_2O = Cr_2O_7^{--} + 2PO_4^{---} + 30H^+ + 22e^-$$

and

$$CrP + 4H_2O = Cr^{+++} + PO_4^{---} + 8H^+ + 8e^-$$

Table 1 lists the corrosion efficiencies that have been measured for both phosphides in a number of solutions. Also listed are the potentials of the anodes (corrected for iR drop) and the nominal current densities in milliamperes per square centimetre. This last column can only be considered as a very approximate measure of the true current density, since many factors (e.g. the roughness and porosity of the surface, possible film-formation, increase of area due to corrosion or physical disintegration, decrease of area due to adhesion of bubbles, etc.) will cause the effective area to differ from the geometrical area.

Inspection of the data in Table 1 will reveal the following facts:

(i) In all solutions studied, the degree of corrosion of CrP is far too serious for any useful electropreparative application. Ni_3P anodes are corroded in neutral solution (they suffer severe chemical attack in acid solutions[3]). At pH 14, Ni_3P anodes appear to resist corrosion perfectly, however this is not likely to have any practical utility in view of the corrosion resistance of nickel itself under such conditions.

TABLE 1

Anode	Solution	% Corrosion Efficiency	Method	Potential versus S.C.E.	Nominal Current Density
CrP	0.5M H_2SO_4	0	2	1.25	3.0
CrP	0.5M H_2SO_4	0	1	1.30	3.4
CrP	0.5M H_2SO_4	0	2	1.33	4.3
Ni_2P	M KOH	0	4		100
Ni_2P	M KOH	0	5		100
Ni_2P	M KOH	0	4		500
CrP	0.5M H_2SO_4	4	2	1.43	4.4
CrP	0.5M H_2SO_4	5	2	1.39	3.4
CrP	M HCl	9	2	1.43	8.7
CrP	M KCl	15	2	1.43	7.8
Ni_2P	M KCl	20	5		100
CrP	M $HClO_4$	20	7	1.62	26
CrP	0.5M H_2SO_4	30	2	1.48	7.5
CrP	0.5M CH_3COOH + 0.5M CH_3COOK	36	2	1.47	5.6
Ni_2P	0.5M Na_2SO_4	40	5		100
CrP	M KOH	(39)	2	0.12	12
"	"	(11)	3	"	"
"	"	50	total	"	"
CrP	satd. KCl	56	6	2.44	1000
CrP	M KOH	(64)	2	0.30	57
"	"	(31)	3	"	"
"	"	95	total	"	"

(ii) The degree of corrosion of CrP anodes in solutions of pH from 0 to 7 depends mainly on the current density (or the potential, which parallels the current density). The effect of anions and of pH are secondary. The corrosion efficiency increases with increasing current density, being about 50% at 100 milliamperes per square centimetre. However, even at extremely high current densities, bubbles are evolved and the corrosion efficiency probably never exceeds about 70%. The corrosion product is $Cr_2O_7^{--}$.

(iii) In neutral solutions, an anode of Ni_2P resists corrosion better than one of CrP. However, a critical comparison is hampered by the different physical states of the two materials.

(iv) In normal solutions of potassium hydroxide, Ni_2P anodes are uncorroded, but corrosion of CrP occurs to both the +3 and +6 states. This corrosion is far more severe than in acidic or neutral solutions, the total corrosion efficiency being about 50% at 10 milliamperes per square centimetre. It would appear that a different corrosion mechanism is operative at pH 14 than in the pH range 0 - 7 and 100% corrosion might be expected to occur at current densities greater than 100 mA cm^{-2} in basic solution.

Table 2 represents an attempt to correlate the results obtained by Wood[1] with those of the present investigation. The construction of the table involves considerable interpolation and the values listed are of little worth, except in illustrating interesting trends in this series of phosphides.

TABLE 2

Corrosion Efficiency at a Current Density of approximately 100 milliamps per square cm.

Phosphide	Acid solution pH = 0	Neutral solution pH = 7	Basic solution pH = 14
FeP	20	30	70
CrP	50	50	100
Fe_2P	30	100	30
Co_2P	100	100	30
Ni_2P	100	30	0

The phosphides in Table 2 form a natural sequence in the order listed. The phosphides at the head of the table possess good resistance to anodic corrosion in acid solution but poor resistance in basic solution; the converse is true at the foot of the table.

Yet another piece of evidence may be cited, supporting the belief that different corrosion mechanisms are operative in basic and acidic solutions. Fig. 3 is the potential -pH diagram[7] for chromium (at 10^{-3} M concentration) compiled from the data given by Latimer[8]. The increasing stability of the +6 state with increasing pH is clearly shown. Yet, in spite of the difference of 1.54 volts in the potential of the Cr(VI)/Cr(III) couple between pH 0 and pH 14, corrosion of CrP in acid solution occurs to the +6 state exclusively while the +3 state is also found in normal alkali.

Some evidence has been collected, based on corrosion experiments with CrP in N H_2SO_4, which strongly suggests the existence of a film at the electrode surface. At potentials of less than 1.35 volts versus S.C.E., a CrP anode in normal sulphuric acid suffers no corrosion (c.f. Table 1). Under these conditions the evolution of oxygen occurs with 100% current efficiency, occuring with a somewhat lower overpotential than at smooth platinum. The stirring resulting from the passage of a stream of nitrogen has no effect on the current, which is quite steady and reproducible at a constant potential: similarly mechanical agitation is without effect. These facts clearly indicate the absence of concentration polarisation. The complete absence of reversibility was demonstrated by the independence of the current upon the concentration of oxygen in the solution. When the anode was subjected to a sudden change in its potential, the current was found to attain its new equilibrium value slowly. The final current was approached from either higher or lower values, depending upon the initial and final potentials, but the final current was a unique function of the potential, being independent of the history of the anode. This behavior would be expected if a film exists at the anode surface, this film being of polymolecular thickness and slowly built up on increasing the potential.

In N H_2SO_4 the onset of corrosion of CrP is not marked by any discontinuity in the current-voltage curve. The system behaves as if a corrosion current becomes added to the existing oxygen current, the latter being unaffected. With increasing potential, both currents increase roughly exponentially, and are about equal in magnitude at the highest

current densities that have been studied. At nominal current densities between about 1.0 and 100 milliamperes per square centimetre, a logarithmic relation between potential and current is obeyed, the value of the parameter b in the Tafel equation,

$$E = a + b \log i$$

being about 0.3 volt. This value is large compared with the usual overvoltage values for b of from 0.05 to 0.2 and would be even larger if the corrosion current were subtracted from the total anodic current. Again, this effect may be explained in terms of a film which increasingly covers a greater fraction of the surface as the potential is increased, thus making the true current density greater than its nominal value.

V. FARADAIC RECTIFICATION

Many investigators[9-14] have observed phenomena associated with the generation of a d.c. potential by the passage of a pure a.c. current across a solution electrode interface. A theoretical treatment for the case of equal concentrations of soluble reductant and oxidant was given by Doss and Agarwal,[12] though the present author believes their derivation to be in error (vide infra).

Doss and Agarwal[10] suggested that the name "redoxokinetic effect" be applied to the phenomenon, because its magnitude is dependent (to some extent) on the kinetics of the oxidation-reduction reaction. However, it is felt that "faradaic rectification" is a more descriptive term which also emphasises the correlation between this effect and the phenomenon appropriately named "faradaic admittance" by Grahame[16].

The charging and discharging of the electrical double layer always provides one path by which alternating current may flow across a solution electrode interface. However, if a redox couple is established at the electrode surface, an additional route is provided by virtue of the occurence of the electrochemical reaction. The dependence of this faradaic component of the a.c. current upon the a.c. potential existing across the interface has been studied by many authors[15-20]. The theoretical treatment below shows that, in addition to this a.c. potential, a constant d.c. potential is also generated by the flow of faradaic a.c. current across the interface.

Theory

Consider an electrode of area A $cm.^2$ across which a pure a.c. current of frequency $w/2\pi$ cycles $sec.^{-1}$ is flowing, i being the magnitude of the faradaic component of this current (in amperes) at time t (seconds). By a convenient definition of zero time, we may express:

$$i = I \cos w t \qquad (1)$$

where I is the amplitude of the a.c. current.

The oxidised form, Ox, of a redox couple is present in solution, its bulk concentration being $\bar{C}$ moles $cm.^{-3}$. The concentration of Ox at any distance, x (cms.), from the electrode surface is denoted by C and C_o is the instantaneous surface concentration. It will be assumed that C_o may be expressed by the Fourier series:

$$C_o = \bar{C}\left[1 + \sum_{j=1}^{j=\infty} \mu_j \cos j\omega t + \sum_{j=1}^{j=\infty} \lambda_j \sin j\omega t\right] \qquad (2)$$

where the μ's and λ's are undetermined coefficients.

If sufficient supporting electrolyte is present in solution and if the frequency is high enough to prevent appreciable convection, diffusion will be the sole mode of transport. Assuming conditions of semi-infinite linear diffusion to exist, Fick's second law:

$$\frac{\partial C}{\partial t} = D \frac{\partial^2 C}{\partial x^2} \qquad (3)$$

must govern the transport of Ox, where D is the diffusion coefficient of Ox in $cm.^2 . sec.^{-1}$. A solution of (3) is required that will satisfy (2) and the additional conditions (4) and (5).

$$C = \bar{C} \text{ for } x = \infty \text{ at all } t \qquad (4)$$

$$(C)_t = (C)_{t+2m\pi/\omega} \text{ for all } x \text{ and integral } m \qquad (5)$$

Such a solution is (compare Randles[17]):

$$\frac{C}{\bar{C}} = 1 + \sum \mu_j \exp\left(-x\sqrt{\frac{j\omega}{2D}}\right) \cos\left(j\omega t - x\sqrt{\frac{j\omega}{2D}}\right) + \sum \lambda_j \exp\left(-x\sqrt{\frac{j\omega}{2D}}\right) \sin\left(j\omega t - x\sqrt{\frac{j\omega}{2D}}\right) \qquad (6)$$

From equation (6) an expression for i may be derived by the application of Fick's first law:

$$i = -nAFD\left(\frac{\partial c}{\partial x}\right)_{x=0} = nAFD\bar{C}\sum(\mu_j + \lambda_j)\sqrt{\frac{j\omega}{2D}}\cos j\omega t$$

$$- nAFD\bar{C}\sum(\mu_j - \lambda_j)\sqrt{\frac{j\omega}{2D}}\sin j\omega t \qquad (7)$$

where F represents the faraday and n is the number of electrons transfered per molecule of Ox reacting. In deriving (7) anodic current has been considered positive. Comparison of (1) and (7) shows that:

$$\mu_j = 0 = \lambda_j \text{ for } j \gg 2 \qquad (8)$$

and:

$$\mu_1 = \lambda_1 = I/nAF\bar{C}\sqrt{2D\omega} \qquad (9)$$

whence (2) becomes:

$$c_0 = \frac{I(\cos \omega t + \sin \omega t)}{nAF\sqrt{2D\omega}} + \bar{C} \qquad (10)$$

Let P be the potential of the electrode, in the absence of current flow, measured in volts versus any convenient reference, the sign being taken in accord with the "European" convention. If an a.c. current of faradaic component i, given by (1), is now passed through the electrode, but flow of d.c. current is prevented, the potential of the electrode becomes $P + \psi + V\cos(\omega t + \theta)$. V and θ are the amplitude and phase angle of the a.c. potential existing across the interface. It is assumed that the electrode potential contains no contribution from

harmonics (i.e. contains no terms in cos $2\omega t$, sin $3\omega t$, etc). Strictly, this is true only in the limit as I approaches zero, however it is approximately true for small values of I. Small values of I (and hence of V and ψ) are assumed henceforth. The d.c. potential ψ is caused by the phenomenon of faradaic rectification and we shall now proceed to derive an expression for it. It is first necessary to specify the chemistry of the redox couple.

The electrode reaction

$$Ox + ne^- = Rd \qquad (11)$$

will be treated first for the case in which Rd is at constant activity. A metal electrode in contact with a solution containing its ions would be an example of this case. For such a system in equilibrium we can write:

$$0 = i = \overleftarrow{i} - \overrightarrow{i} = nAFk \exp\left(\frac{n(1-\alpha)FE}{RT}\right) - nAFk\bar{C} \exp\left(\frac{-n\alpha FE}{RT}\right) \qquad (12)$$

where $\overleftarrow{i}$ and $\overrightarrow{i}$ are the individual currents corresponding to the reverse and forward directions of (11). The gas constant and the absolute temperature are denoted by R and T and α is the symmetry factor or transfer coefficient for the electrode reaction, taking some value between zero and unity. The term k is a rate constant, being the actual rate of both reverse and forward reactions when $\bar{C} = 1$. E is defined by $E = P - P_0$, P_0 being the value of P when $\bar{C} = 1$.

Upon application of a.c., $\overleftarrow{i}$ and $\overrightarrow{i}$ are no longer equal, since now:

$$\overleftarrow{i} = nAFk \exp\left(\frac{n(1-\alpha)F}{RT}\left[E + \psi + V\cos(\omega t + \theta)\right]\right) \qquad (13)$$

and:

$$\vec{i} = nAFkC_0 \exp\left(\frac{-L\alpha F}{RT}\left[E + \Psi + V\cos(\omega t + \theta)\right]\right) \qquad (14)$$

where C_0 is given by (10). Now if V is small compared with $Rt/n\alpha F$, Ψ will be still smaller and the following approximations will be valid:

$$\exp\left(\frac{-n\alpha F}{RT}\Psi\right) = 1 - \frac{n\alpha F}{RT}\Psi \qquad (15)$$

$$\exp\left(\frac{-n\alpha FV}{RT}\cos(\omega t + \theta)\right) = 1 - \frac{n\alpha FV}{RT}\cos(\omega t + \theta) + \frac{n^2\alpha^2F^2V^2}{2R^2T^2}\cos^2(\omega t + \theta)$$

$$= 1 + \frac{n^2\alpha^2F^2V^2}{4R^2T^2} - \frac{n\alpha FV}{RT}\cos\theta\cos\omega t + \frac{n\alpha FV}{RT}\sin\theta\sin\omega t \qquad (16)$$

and similar approximations with $(1 - \alpha)$ replacing $(-\alpha)$. The final step in approximation (16) is made by neglecting the harmonic term in $\cos(2\omega t + 2\theta)$. The worst error introduced by these approximations is about 2.5% if $V \leqslant RT/2n\alpha F$, which is $V \leqslant 12$ milli-volts at 25°C for $n\alpha = 1$. If these approximations are inserted into (13) and (14), A eliminated by means of (12), small or harmonic terms neglected and finally (14) subtracted from (13), the following results:

$$\frac{\overleftarrow{i} - \overrightarrow{i}}{nAFk(\bar{C})^{1-\alpha}} = \frac{n^2F^2V^2}{4R^2T^2}(1 - 2\alpha) + \frac{nF}{RT}\psi + \frac{\alpha\, IV}{2A\bar{C}\sqrt{2D\omega}}(\cos\theta - \sin\theta)$$

$$+ \cos\omega t\left(\frac{nFV}{RT}\cos\theta - \frac{I}{nAF\bar{C}\sqrt{2D\omega}}\right)$$

$$- \sin\omega t\left(\frac{nFV}{RT}\sin\theta + \frac{I}{nAF\bar{C}\sqrt{2D\omega}}\right) \qquad (17)$$

Since $\overleftarrow{i} - \overrightarrow{i} = i$, equations (1) and (17) must yield identical expressions for the value of the instantaneous faradaic current. Hence, equating the coefficient of $\sin\omega t$ in (17) to zero and that of $\cos\omega t$ to I, we obtain:

$$\cos\theta = -(1 + 2H) \qquad (18)$$

and:

$$V = \frac{IRT}{n^2AF^2\bar{C}\sqrt{D\omega}}(1 + 2H + 2H^2)^{\frac{1}{2}} \qquad (19)$$

where:

$$H = \frac{-\alpha}{k}\sqrt{\frac{D\omega}{2}} \qquad (20)$$

The time-independent term on the right hand side of (17) must equal zero (this corresponds to the restriction that no d.c. current is allowed to flow). From this condition, by means of (18) and (19), the following expression for ψ is derived:

$$\psi = -\frac{nFV^2}{2RT}\left(1/2 - \frac{\alpha(H + 2H^2)}{1 + 2H + 2H^2}\right) \qquad (21)$$

This equation has two interesting limiting cases. If $k \ll \bar{C}^{-\alpha}\sqrt{D_\omega}$,

$$\Psi = -\frac{nFV^2}{2RT}\,(1/2 - \alpha) \tag{22}$$

whereas if $k \gg \bar{C}^{\alpha}\sqrt{D_\omega}$,

$$\Psi = -\frac{nFV^2}{4RT} \tag{23}$$

For intermediate values of k, Ψ is a symmetrical sigmoid function of log H as depicted in Fig. 4, the point of inflection being at $H = 1/\sqrt{2}$.

If (11) represents a redox couple both components of which are in solution, having equal bulk concentrations, $\bar{C}$, then it has been shown by Randles[17] that the surface concentrations of Ox and Rd obey the relationship:

$$(C_o)_{Ox} + (C_o)_{Rd} = 2\bar{C} \quad \text{if } D_{Ox} = D_{Rd} \tag{24}$$

With this additional relationship, a derivation may be carried out which is strictly analogous to the one given above. The results are as follows:

$$\cot\,\theta = -(1 + 2J) \tag{25}$$

$$V = \frac{2IRT}{n^2AF^2\bar{C}\sqrt{D_\omega}}\,(1 + 2J + 2J^2)^{\frac{1}{2}} \tag{26}$$

$$\Psi = \frac{(\alpha - 1/2)nFV^2}{2RT}\left(\frac{J + 2J^2}{1 + 2J + 2J^2}\right) \tag{27}$$

where:

$$J = \frac{1}{2k}\sqrt{\frac{D\omega}{2}} \tag{28}$$

The expression (27) differs from the result obtained by Doss and Agarwal[12] for the same problem. The present author believes that the approximations that were made in their derivation were too drastic. The expression for Ψ takes a simpler form than (27) in terms of the amplitude of the faradaic current, thus:

$$\Psi = \frac{(\alpha - 1/2)\, I^2RT}{n^3F^3A^2C^2k}\left(\sqrt{\frac{2}{D\omega}} + \frac{1}{k}\right) \tag{29}$$

Equivalent Circuit

The properties of an electrode surface with respect to faradaic a.c. cannot be depicted in terms of a circuit consisting of resistors and condensers, unless peculiar frequency-dependences are ascribed to these components. However, the properties of a "Warburg impedance", introduced by Grahame[16] are very useful in this respect. The properties of this circuit element are such that its impedance is inversely proportional to the square root of the frequency of the a.c. current. This current leads the voltage by a constant angle of $\pi/4$ radians.

If the current $i = I \cos \omega t$ is passed through the series combination of a resistor and a Warburg impedance, the potential across the pair is readily shown to be:

$$\frac{W}{\sqrt{\omega}}\left(1+\frac{r}{W}\sqrt{2\omega}+\frac{r^2\omega}{W^2}\right)^{1/2}\cos\omega t-\operatorname{arccot}\left(1+r\sqrt{2\omega}/W\right) \quad (30)$$

where r and $W/\sqrt{\omega}$ are the impedances of the individual element. Comparison of (30) with equations (18) - (21), shows that the faradaic properties of the solution electrode interface are accurately represented by the circuit shown in Figure 5, where the -W- symbol represents the Warburg impedance[16] and the battery symbol represents a source of d.c. potential in the sense shown, but a short-circuit as far as a.c. is concerned. The magnitudes of the components of the equivalent circuit are:

$$\frac{W}{\sqrt{\omega}}=\frac{RT}{n^2AF^2\sqrt{2}\sqrt{D_0}} \quad (31)$$

$$r=\frac{RT}{n^2AF^2k(C)^{-1}-\sigma} \quad (32)$$

$$P+\psi=P-\frac{RT^2}{2F^2}\left(1/2-\frac{\sigma\left(H+2H^2\right)}{1+2H+2H^2}\right) \text{ where } H=\frac{r}{W}\sqrt{\frac{W}{2}} \quad (33)$$

The elements in Fig. 5 are drawn at angles such that the diagram also represents a voltage vector diagram.

The elements connected by dashed lines in Fig. 5 represent an alternative method, due to Randles[17], of representing the properties of the Warburg impedance. In Randles' notation:

$$R_p - r = W/\sqrt{2\omega} = 1/\omega C_p \qquad (34)$$

Expressions for R_p and C_p may be readily derived from (31), (32) and (34); they will be found to differ by factors of $\sqrt{2}$ from the expressions deduced by Hillson (15) for the same problem. In the present author's opinion, Hillson's derivation is in error by this factor. Similar treatment of equations (25), (26) and (28), for the case of equal concentrations of Ox and Rd, yields expressions for R_p and C_p identical with those of Randles[17].

In the construction of the complete equivalent circuit of the cell, account must be taken of the double layer capacity, C_d, which introduces a reactance in parallel with the faradaic impedance of the interface, and of the necessary presence in the cell of a second electrode. If this second electrode is of the same material as the first, its interface will have a similar equivalent circuit to that shown in Fig. 5. The two electrodes are linked by a pure resistance, R_s, the ohmic resistance of the intervening solution, and hence the entire cell is electrically analogous to the circuit which is depicted vectorially in Figure 6.

If the area of the second electrode is made very much larger than that of the first, equations (31) and (32) show that the faradaic impedance will assume a negligibly small value. The non-faradaic reactance is also inversely proportional to electrode area, so that for the large electrode, $W' = r' = 1/C_d' = 0$, and these circuit elements may be ignored. Equation (21) shows that ψ' is not an explicit function of the area of the second

electrode. However, ψ' is proportional to the square of V', the a.c. potential developed across the interface, and this latter will tend to zero as the area of the second electrode is increased. Thus, for a cell containing similar electrodes of very different areas, the equivalent circuit reduces to that shown in Figure 7, the d.c. potentials P + ψ and P (in the opposite sense) having been combined into a single, measurable element, ψ.

Applications

As has been demonstrated above, the d.c. potential, ψ, is proportional to the square of the a.c. potential, V, produced across the interface. The constant of proportionality is a function of known constants (R, D, etc.), known variables (ω, $\bar{C}$, etc.) and certain, often unknown, parameters (α, k, n) of the system. Hence, experimental measurement of ψ as a function of V^2 provides a method for the determination of these parameters.

The potentialities of the method are most clearly demonstrated by Fig. 4. (This figure applies only, of course, to the reaction considered first, i.e. the n electron discharge of a soluble molecule of Ox to a species Rd at constant activity. However, similar diagrams may be readily constructed for any other type of electrochemical reaction). Experimental variation of such factors as frequency, concentration and temperature will vary H and so extensive regions of the curve in Fig. 4 may be determinable; in fortunate circumstances, the whole curve might be recorded.

The upper limit of ψ (corresponding to large C and large w, but small k - right hand side of Fig. 4), is seen to be very sensitively dependent on the magnitude of α and hence the investigation of this region offers an excellent method for the evaluation of the symmetry factor of the electrode reaction. This fact was first realized by Doss and Agarwal[12], who used experimental data on the Fe^{++}, Fe^{+++} (equimolar) / Pt electrode to calculate the symmetry factor (transfer coefficient) of the exchange reaction. However, it is felt that their data are in error because of failure to take account of the a.c. potential developed across the solution resistance, R_s, which must be subtracted, vectorially, from the a.c. cell potential, to obtain the true interfacial potential, V.

From the inflection point of the rising portion of the graph of ψ/V^2 versus the logarithm of frequency (at constant concentration), or in some similar fashion, it is possible to determine k, the rate constant of the electrode reaction. This parameter is also calculable from measurements of the faradaic impedance of the electrode[15-19] and the greater inherent accuracy of the bridge techniques used in such investigations will be reflected in a more precise evaluation of k than by measurement of the degree of faradaic rectification. However, the latter method offers a unique advantage over the classical method when applied to solid electrodes. Whereas the calculation of k from impedance data requires a knowledge of the electrode area[17,18], equation (21) shows that ψ/V^2 is independent of A.

Fig. 4 shows that measurement at the lower limit of ψ will enable n to be obtained. Though this quantity is rarely in doubt (for such a simple reaction as (11)), its accurate evaluation will provide confidence in the method.

For complex electrode reactions, study of faradaic rectification may assist in the determination of the reaction mechanism. Thus if a complex reaction is representable by the equivalent reaction pair[5]:

$$n\ Ox + n\beta\ e^- = p\ Rd - n(1-\beta)e^- \qquad (35)$$

where β is not necessarily a symmetry factor. For such a reaction, it may be shown that:

$$\psi = -\frac{nFV^2}{2RT}\left(1/2 - \frac{\beta(X + 2X^2)}{1 + 2X + 2X^2}\right) \qquad (36)$$

where:

$$X = \sqrt{\frac{\nu D}{2}}\ \frac{D^{(1-m+\beta m)}}{m^2 k} \qquad (37)$$

(c.f. equations (21) and (20), to which (36) and (37) reduce when $n = 1$ and $\beta = \alpha$.). It will be seen that study of the degree of faradaic rectification offers a method for the evaluation of n and β, which may greatly assist in the establishment of the reaction mechanism[5].

Hitherto it has been assumed that the flow of d.c. current is prevented, e.g. by the presence of a blocking condenser. Current will flow if this is not the case and the direction of current flow will be in accord with the sign of ψ. A glance at Fig. 4 will show that ψ is usually

negative; that is to say that if two electrodes, of copper for example, are immersed in a solution containing copper ions and connected by a wire in which an a.c. is induced, the smaller electrode will tend to assume a slight negative charge with respect to the larger. Current will flow, accompanied by a deposition of copper at the large electrode at the expense of the small. A comparable situation would arise if a massive piece of copper was totally immersed in the solution, in the presence of an a.c. field, the large and small electrodes resulting from different grain sizes at the metal surface. Even though no net dissolution of copper would occur, a pitting and roughening of the surface would be expected. It is interesting to speculate on whether such an effect contributes any responsibility for the agravation of metallic decay in the vicinity of a.c. installations that has often been observed by corrosion engineers.

VI. RECTIFICATION EXPERIMENTS

The limitation to the accurate determination of ψ/V^2 is imposed, not by the measurement of ψ which is a comparatively simple matter, but by the difficulty in determining V. This is partly because of the exponent, but mainly because V cannot be measured directly. V is defined as the amplitude of the a.c. potential existing across the interface, i.e. across the triangular network in Fig. 7. An a.c. millivoltmeter may be employed to measure V_1, the total potential across the cell, but this contains a contribution V_s from the passage of the a.c. current through R_s, and the vectorial subtraction cannot be carried out without a

knowledge of the phase angle between V_s and V. Instead of measuring this phase angle, an alternative procedure was adopted which is illustrated by Figure 8, a semi-vectorial diagram of the essential circuitry of the experimental apparatus. A resistor, R, is placed in series with the cell and its magnitude is adjusted to be exactly equal to R_s. The measurable potential, V_s, across R is thus equal in both magnitude and phase to V_s. The total potential drop, V_3, across the series combination of R and the cell is also determined. It will be seen from Fig. 8 that the vectors V_1 and V_2 form the adjacent sides of a rhomboid, of which V and V_3 are the diagonals. Geometrical considerations relate the lengths of the sides and diagonals of a rhomboid in such a manner that:

$$V^2 = 2V_1^2 + 2V_2^2 - V_3^2 \qquad (38)$$

This relationship was used to measure V^2.

Equation (38) shows that the determination of V^2 is the more accurate, the smaller the value of R_s. This consideration was paramount in dictating the design of the apparatus shown in Figure 9, and the choice of supporting electrolyte. The cell employs mercury electrodes, the large electrode being simply a pool on the floor of the cell. The small electrode, a slightly flattened hemisphere of mercury, of a few $mm.^2$ area, "balanced" on the end of the S-shaped siphon tube. This electrode is established by adding mercury dropwise at B (Fig. 9), until the mercury just fails to overflow. With practice, it is possible to reproduce the area of the small electrode to give an uncertainty of about 0.1 ohm in 3.0 ohms

(a typical value for R_s); this reproducibility is not, however, required, since the resistance R was always adjusted to the new value of R_s after reforming the surface of the small electrode.

The sinusoidal signal used in the measurement of faradaic rectification is produced by the audio-frequency oscillator O1 (Fig. 9), a "Low Distortion Oscillator", manufactured by General Radio Co. (Type 1301A). This precision oscillator generates any one of 27 standard frequencies from 20 c/s. to 15 kc/s., of continuously variable voltage. The isolation transformer O2 was a "Low Harmonics Transformer" (Type 578B of General Radio Co.), serving also as a 4X step-up transformer. The condenser C1 (Cornell-Dubilier decade capacitor unit, usually set at 1.0 microfarad) serves to prevent the flow of d.c. current, while the choke L (8 henry, low resistance a.f. choke) prevents the a.c. signal from being shorted by the potentiometer used to measure ψ. The parallel network of R1 and R2 (both noninductively wound precision decade resistors) constitutes R, the resistor that is set equal to R_s, the solution resistance of the cell. The measurement of R_s involves the use of the auxiliary r. f. oscillator, O2 (Heathkit, model AG-8), a sine wave generator of continuously variable frequency. The total impedance of the cell was measured by switching in O2, via the r.f. isolation transformer T2, and adjusting R until V_1 and V_2 are equal; the impedance is then equal to R. This measurement was made at 40 kc/s and at 56.6 kc/s and extrapolated to infinite frequency by means of the relationship (exact for a resister and capacitor in series):

$$2(Z)_{56.6k} - (Z)_{40k} = (Z)_{\infty} = R_s \qquad (39)$$

The resistors R1 and R2 were then adjusted such that their harmonic mean was equal to the value of R_s calculated by (39). When switch S2 had been opened, the apparatus was completely adjusted for the measurement of Ψ and V^2.

To avoid the use of three a.c. meters as shown in Fig. 8, a four-bank, four position switch S1 was used in conjunction with a single a.c. millivoltmeter, M (Heathkit, model AV-2). This meter has a sensitivity of 10 millivolts r.m.s. for full scale deflection, together with several less sensitive scales. It was found to have a flat frequency response over the range of operation of O1 and was calibrated to read directly in square millivolts of amplitude. The first three positions of the switch S1 enable the terms V_1^2, V_2^2 and V_3^2 to be measured; the fourth commons the mercury electrodes, enabling their common potential to be measured versus the reference electrode, REF. A cathode ray oscilloscope (Dumont model 304H) was permanently connected in series with M, enabling the a.c. signals to be monitored visually, to give assurance that the signals were undistorted. In the first three positions of switch S1, the mercury electrodes are connected through L to the potentiometer, POT., enabling the potential Ψ to be measured. This potentiometer was constructed on the Poggendorff principle, having a total range of $\pm$ 15 millivolts. The slide-wire drum could be readily adjusted to one microvolt, but the accuracy was limited by the galvanometer (Rubicon, mirror-in-box type) which has a voltage sensitivity of 13 microvolts/millimeter.

Table 3 shows the results of 31 experiments with the apparatus, employing a 1.0 millimolar ($\bar{C} = 10^{-6}$) of mercurous ion, Hg_2^{++} in 5.0 M perchloric acid at 25°C. These results cover a wide range of frequencies and a.c. potentials. Excepting the results obtained under the most extreme conditions (there are diverse reasons for the belief that erroneous values of ψ will be obtained if either ω or V is too large or too small), all the observed values of $4RT\psi/FV^2$ lie between -1.7 and -2.1, with most lying within 0.08 of the mean value, -1.85. There is no trend with frequency of the term $4RT\psi/FV^2$, showing that in the range of experimental conditions, equation (21) for ψ always assumes one its limiting, frequency-independent forms (22) or (23). From the magnitude of the effect, it is clear that it is equation (23) that is operative and that the experimental value of $4RT\psi/FV^2$, -1.85, is an approximation to the true value of -n, 2.0. Many causes for this 7% discrepency may be surmised, but the operative cause is unknown. The small, unexpected positive trend in ψV^{-2} with increasing V shown in table 3 for the results at 75 c/s, appears to be a real effect, though it remains unexplained. However, within the most useful range of V, between 4 and 10 millivolts, the trend is not apparent.

The results in table 3 refer to the lower limit shown in Fig. 4. It would appear that $\log H < -2$, from which the approximate lower limit $k > 0.05$ may be calculated. Attempts were made to increase H and so obtain points on the rising portion of Fig. 4, both by increasing $\bar{C}$ and by decreasing k (by lowering the temperature and by the addition of gelatin[17]): these were unsuccessful.

VII. REFERENCES

(1) D. W. Wood, Ph.D. Thesis, University of Illinois (1953).

(2) D. W. Wood, University Microfilms (Ann Arbor, Michigan) Publ. No. 5251 (1953).

(3) S. S. Hsu, P. N. Yocom and T. C. C. Cheng, Quarterly Status Reports to the Office of Naval Research, This Contract (1954-55).

(4) K. B. Oldham, J. Amer. Chem. Soc., in press, (1955).

(5) P. Cazeneuve, Compt. rend., 131, 346 (1900).

(6) F. Feigl, "Qualitative Analysis by Spot Tests", Elsevier Publishing Company, New York, p. 128 (1947).

(7) P. Delahay, M. Pourbaix and P. van Rysselberghe, J. Chem. Educ., 27, 683 (1950).

(8) W. M. Latimer, "Oxidation States.....", Prentice Hall Company, New York, (1950).

(9) LeBlanc and Schick, Z. physik. Chem., 46, 213 (1903).

(10) K. S. G. Doss and H. P. Agarwal, J. Sci. industr. Res. (India) 9B, 230 (1950).

(11) Idem, Proc. Ind. Acad. Sci., 34, 229 (1951).

(12) Idem, ibid, 34, 263 (1951).

(13) H. P. Agarwal, J. Sci. Soc. Harcourt Butler Tech. Inst. and Indian Inst. of Sugar Tech. Kanpur, 2, 35 (1953).

(14) H. P. Agarwal and Y. K. Gupta, ibid, 2, 52 (1953).

(15) P. J. Hillson, Trans. Faraday Soc., 50, 385 (1954).

(16) D. C. Grahame, J. Electrochem. Soc., 99, 370C (1952).

(17) J. E. B. Randles, Discus. Faraday Soc., 1, 11 (1947).

(18) H. Gerischer, Z. physik. Chem., 198, 286 (1951).

(19) P. Delahay, "New Instrumental Methods in Electrochemistry", Interscience publishers Inc., New York, N. Y., p (1954).